https://doi.org/10.5194/se-2022-9
Preprint. Discussion started: 2 February 2022

Tectonic evolution of the Indio Hills segment of the San Andreas fault in southern California

Jean-Baptiste P. Koehl[1,2,3,4], Steffen G. Bergh[2,3], Arthur G. Sylvester[5]
1) Centre for Earth Evolution and Dynamics, (CEED), University of Oslo, N-0315 Oslo, Norway.
2) Department of Geosciences, UiT The Arctic University of Norway in Tromsø, N-9037 Tromsø, Norway.
3) Research Center for Arctic Petroleum Exploration (ARCEx), UiT The Arctic University of Norway.
4) CAGE – Centre for Arctic Gas Hydrate, Environment and Climate, UiT The Arctic University of Norway.
5) Department of Earth Science, University of California, Santa Barbara, USA.
Correspondence: jeanbaptiste.koehl@gmail.com

Abstract

Transpressional uplift domains of inverted Miocene–Pliocene basin fill along the San Andreas fault zone in Coachella Valley, southern California, are characterized by fault linkage and segmentation and deformation partitioning. The Indio Hills wedge-shaped uplift block is located in between two boundary fault strands, the Indio Hills fault to the northeast and the Banning fault to the southwest, which merge to the southeast. Uplift commenced about 2.2–0.76 million years ago and involved progressive fold and faulting stages caused by a change from distributed strain to partly partitioned right-slip and reverse/thrust displacement on the bounding faults when approaching the fault junction. Major fold structures in the study area include oblique, right-stepping, partly overturned *en echelon* macro-folds that tighten and bend into parallelism with the Indio Hills fault to the east and become more open towards the Banning fault to the west, indicating an early and close relationship of the macro-folds with the Indio Hills fault and a late initiation of the Banning fault. Sets of strike-slip to reverse step-over and right- and left-lateral cross faults and conjugate kink bands affect the entire uplifted area, and locally offset the *en echelon* macro-folds. Comparison with the Mecca Hills and Durmid Hills uplifts farther southeast in Coachella Valley reveals notable similarities, but also differences in fault architectures, spatial and temporal evolution, and deformation mechanisms.

Introduction

This paper describes and evaluates structural patterns of the Indio Hills uplift in the northwestern part of Coachella Valley along the San Andreas Fault Zone (SAFZ; Fig. 1), where the fold–fault architecture, evolution, and partitioning of deformation compared to

https://doi.org/10.5194/se-2022-9
Preprint. Discussion started: 2 February 2022

Solid Earth Discussions

Mecca Hills and Durmid Hills are not well understood (e.g., Keller et al., 1982, Parrish, 1983; Dibblee and Minch, 2008). The main goal of this study is to analyze internal macro- and meso-scale folds and related faults and to outline the kinematic evolution in relation to major SAFZ-related fault strands in the area (Fig. 1: Keller et al., 1982; Guest et al., 2007). These include the Banning fault along the southwest flank of the Indio Hills, thought to correspond to the main SAFZ in Mecca Hills and Durmid Hills (Janecke et al., 2018), and the Indio Hills fault in the northeast (Allen, 1957; Tyley, 1974; Fig. 1), which merges with the Eastern California Shear Zone to the north and with the Banning fault in the southeast. The progressive tectonic evolution model for the Indio Hills uplift is then compared and correlated with other major uplifts and SAFZ-related fault strands along strike in the Mecca Hills and Durmid Hills (Sylvester and Smith, 1987; McNabb et al., 2017; Janecke et al., 2018; Bergh et al., 2019). We also discuss briefly the northwestward continuation of the Indio Hills fault into the East California Shear Zone (Dokka and Travis, 1990a, 1990b; Thatcher et al., 2016). The variable fault and fold architectures and associated ongoing seismic activity in these uplift areas underline the need for persistent along-strike studies of the SAFZ to characterize the fundamental geometry, resolve the kinematic development, and correlate regionally major fault strands (cf. Janecke et al., 2018). Such studies are essential to explain the observed lateral variations in fold and fault architectures and to resolve mechanisms of transpression, fault linkage, and areal segmentation in continental transform settings.

Geological setting

The Coachella Valley segment of the SAFZ in southern California is expressed as three uplifted, right-lateral, transpressional domains located in the Indio Hills, Mecca Hills, and Durmid Hills (Fig. 1; Sylvester, 1988). These domains comprise thick successions of Miocene–Pliocene sedimentary strata uplifted and deformed in Pleistocene time due to oblique convergence of the Pacific and North American plates and transform movements along the SAFZ and related faults (e.g., Spotila et al., 2007; Atwater and Stock, 1998; Dorsey et al., 2011). Recent structural studies in the Mecca Hills (McNabb et al., 2017; Bergh et al., 2019), and Durmid Hills at the southern termination of the SAFZ (Janecke et al., 2018), show that individual fault strands are linked, and that the deformation splits into abruptly changing fold and fault geometries (Fuis et al., 2012, 2017).

https://doi.org/10.5194/se-2022-9
Preprint. Discussion started: 2 February 2022

Solid Earth Discussions

Stratigraphy of the Indio Hills and adjacent areas

The Indio Hills culmination is an inverted Miocene–Pliocene sedimentary basin lying upon Mesozoic granitic basement rocks, which we regard as analogous to the Mecca rift basin farther southeast (Keller et al., 1982; Damte, 1997; McNabb et al., 2017; Bergh et al., 2019). In the Mecca basin,alluvial, fluvial and lacustrine deposits of the Mecca and Palm Springs formations are truncated unconformably by the late Pleistocene–Quaternary Ocotillo Formation (Dibblee, 1954; Sylvester and Smith, 1976, 1987; Boley et al., 1994; Rymer, 1994; Sheridan et al., 1994; Sheridan and Weldon, 1994; Winker and Kidwell, 1996; McNabb et al., 2017). Similar uplifted strata at Durmid Hills (Fig. 1) belong to the Pliocene–Pleistocene Borrego Formation, and are overlain by mid/upper Pleistocene deposits of the Brawley and Ocotillo formations (Dibblee, 1997; Herzig et al., 1988; Lutz et al., 2006; Kirby et al., 2007; Dibblee and Minch, 2008).

Leuco-granitic basement rocks crop out near gently SW-dipping conglomerates along the northeastern flank of the Indio Hills, near the trace of the Indio Hills fault (Fig. 2). Despite the proximity of the conglomerates with disconnected granite outcrops, the contact itself is not exposed. The conglomerates are the lowermost stratigraphic unit exposed in the Indio Hills and are characterized by a succession of meter-thick beds of very coarse, poorly sorted blocks of gneissic and granitic basement rocks more than a meter in size. We consider the conglomerates as stratigraphic equivalents to the Miocene–Pliocene Mecca Formation in the Mecca Hills (Dibblee, 1954; Sylvester and Smith, 1987; Bergh et al., 2019). Up-section toward the southwest the conglomerate gradually turns into coarse-grained sandstone, which defines the transition from the Mecca Formation to the lower Palm Spring Formation.

The Palm Spring Formation in the Indio Hills consists of moderately- to well-consolidated alluvial fan deposits (Parrish, 1983), with some interbedded gypsum layers and red-colored calcareous mudstone, as in the Mecca Hills (Sylvester and Smith, 1987). The main rock types include beds of light-colored, medium- to coarse-grained sandstone, gray–brown silty sandstone, and dark biotite-rich mudstone. The increase in silt–clay toward the Banning fault was also recorded in the Mecca Hills and may indicate a transition from the lower to the upper member of the Palm Spring Formation (Bergh et al., 2019).

The transition between the lower and upper members of the Palm Spring Formation in the Mecca Hills is an angular unconformity that signals further steps in uplift and inversion of the Mecca basin (McNabb et al., 2017; Bergh et al., 2019). In the Indio Hills, however, the nature of the transition between the lower and upper member of the Palm Spring Formation and the presence of an angular unconformity is unknown. Absolute dating revealed an age of

https://doi.org/10.5194/se-2022-9
Preprint. Discussion started: 2 February 2022

3.7-2.6 Ma (mid–late Pliocene) and 2.8–1.0 Ma (late Pliocene–mid Pleistocene) for the lower and upper member of the Palm Spring Formation, respectively, in the Mecca Hills, based on reversed magnetic polarity data (Chang et al.,1987; Boley et al., 1994), and sediment accumulation rate estimates (McNabb, 2013). Inversion of the Mecca basin started and lasted beyond the early/mid Pleistocene (< 0.76 Ma). Additional dating limits on the transpressional uplift in Mecca Hills and Durmid Hills emerges from the involvement of the 0.765 million year old Bishop Ash layer (Sarna-Wojcicki et al., 2000; Zeeden et al., 2014) in the uppermost members of the Palm Spring Formation (McNabb et al., 2017; Bergh et al. 2019; Janecke et al., 2018). In contrast to other uplift areas in Coachella Valley, the Ocotillo Formation has not been mapped in the Indio Hills, but rather is deposited on the flank northeast of the Indio Hills fault, and southwest of the Banning fault (Figs. 1 and 2), indicating that the Ocotillo Formation was either not deposited, or eroded in the area of uplift.

Tectonic Culminations

Indio Hills

The Indio Hills are a WNW–ESE–trending tectonic culmination situated in a small restraining bend northeast of the main SAFZ trace (Figs. 1 and 2). The culmination is located along strike about 25–50 kilometers northwest of the Mecca Hills and Durmid Hills, and to the southeast of the major left bend in the SAFZ trace near San Gorgonio Pass (Dair and Cooke, 2009). The Miocene–Pliocene proto-SAFZ strata are structurally bounded north of the Coachella Valley by a low-topographic relief SAFZ segment and several left-slip splay faults that merge into the uplifted San Bernardino and San Jacinto fault strands (Bilham and Williams, 1985; Spotila et al., 2007), and the West Salton detachment fault in the southwest (Dorsey et al., 2011).

The southeastern end of the Indio Hills is an uplifted domain of deformed strata of the Mecca and Palm Spring formations situated in between the Banning and Indio Hills fault (Fig. 2). The Banning fault corresponds to a major oblique strike-slip fault segment at the eastern end of San Gorginio Pass (Matti et al., 1985; Morton et al, 1987) and is easily traced to Indio Hills (Figs. 1 and 2) since its main fault gouge provides preferential pathways for ground water flow and growth of wild palm trees along strike.

The Indio Hills fault was mapped north of the study area (Parrish, 1983; Dibblee and Minch, 2008) extending into the Landers–Mojave Line (Nur et al., 1993a, 1993b), a NNW–SSE-striking right-lateral fault system extending hundreds of kilometers northward from the southeastern Indio Hills into the East California Shear Zone and related fault segments such

https://doi.org/10.5194/se-2022-9
Preprint. Discussion started: 2 February 2022

as the Calico and Camp Rock faults (Fig. 1; Dokka et al., 1990a; Nur et al. 1993b). The Indio Hills fault may correspond to a major fault splay of the SAFZ (Dokka and Travis, 1990a, 1990b; Thatcher et al., 2016). Farther southeast, however, the attitude and geometry of the Indio Hills fault remain elusive, and the fault dies out or merges either with the Banning fault, the Skeleton Canyon fault, and/or the Painted Canyon fault in the Mecca Hills (Fig.1).

The transpressional character of the Indio Hills uplift was suggested by Parrish (1983) and Sylvester and Smith (1987), but modern data remain scarce, and detailed structural analyses have not been published from this segment of the SAFZ. An exception is the study of Keller et al. (1982) focusing on an area northwest of our study area and aimed at investigating the tectonic geomorphology near the intersection of the Banning and Mission Creek faults (Fig. 1; Blisniuk et al., 2021). Besides studying soil profiles, offset drainage systems, and recent (a few thousand years old) displacement along the SAFZ, their study called attention to a strong dominance of gently plunging and upright macro-folds in bedrock strata along the Mission Creek fault and at the southeastern end of the Banning fault where these faults merge. Their study showed that bends and steps along the main fault traces were consistently located near brittle fault segments and zones of uplift.

Mecca Hills

Farther south, the Mecca Hills uplift was previously defined as a classic flower-structure (Sylvester and Smith, 1976, 1987; Sylvester, 1988), in which all folds and faults formed synchronously and merged at depth. Recent analyses indicate that a modified flower-like structure, consisting of a steep SAFZ fault core zone to the southwest, a surrounding off-fault approximately one–two kilometers wide damage zone expressed by *en echelon* folds and faults oblique to the SAFZ (including left-slip cross faults), steeply plunging folds, and SAFZ-parallel fold and thrust belt features (including right- and left-slip and oblique-reverse faults) formed in kinematic succession (Bergh et al., 2014, 2019). In addition to the steep SAFZ, two other, major NW–SE-striking faults exist in the Mecca Hills (Fig. 1). One is the Skeleton Canyon fault, which initiated as a steep SAFZ-parallel strike-slip fault and was reactivated as a reverse and thrust fault dipping gently northeastwards in the late kinematic stages. The other is the Painted Canyon fault, which marks the former Miocene–Pliocene basin-bounding normal fault and is now reactivated as a NE-directed thrust fault with dip to the southwest (Bergh et al., 2019). The polyphase evolution and reactivation of internal oblique, step-over faults, and SAFZ-parallel faults, were explained by a series of successive–overlapping events involving a change from distributed, locally partitioned, into fully partitioned strain in a changing, oblique-plate convergence regime (Bergh et al., 2019).

https://doi.org/10.5194/se-2022-9
Preprint. Discussion started: 2 February 2022

Durmid Hills

The Durmid Hills are an elongate ridge that parallels the main strand of the SAFZ at the south edge of the Salton Sea in Imperial Valley (Fig. 1) and is aligned to the south with the Brawley seismic zone, an oblique, transtensional rift area with particularly high seismicity (Lin et al., 2007; Hauksson et al., 2012; Lin, 2013). The main fault strand (mSAF) is located on the northeast side of the Durmid Hills (Janecke et al., 2018) and has been thoroughly studied (Dibblee, 1954, 1997; Babcock, 1969, 1974; Bilham and Williams, 1985; Bürgmann, 1991; Sylvester et al., 1993; Lindsey and Fialko, 2013). The rocks southwest of the mSAF consist of highly folded Pliocene–Pleistocene deposits (Babcock, 1974; Bürgmann, 1991; Markowski, 2016) bounded to the southwest by the subsidiary East Shoreline Fault strand of the SAFZ, whereas the formations are much less deformed northeast of the mSAF (Janecke et al., 2018). The overall structure (Fig. 1) resembles a right-lateral strike-slip duplex (Sylvester, 1988), but the geometry is not fully consistent with a duplex model due to abundant left-lateral cross faults and internal block rotations. Instead, the Durmid Hills structure was interpreted as a ladder structure (Janecke et al., 2018), as defined by Davis (1999) and Schulz and Balasko (2003), where overlapping, E–W- to NW–SE-striking step-over faults rotated along multiple connecting cross faults. The one–three kilometers wide Durmid ladder structure consists of multiple internal, clockwise-rotating blocks bounded by major *en echelon* folds and right- and left-lateral cross faults in between the right-slip mSAF and Eastern Shoreline Fault strand, indicating a complex termination of the SAFZ around the Brawley Seismic Zone to the southeast (Fig.1).

Methods and data

In the present study, we used high-resolution Google Earth DEM images and aerial photographs (© Google Earth 2011) as basis for detailed field and structural analyses in the Indio Hills (Fig. 2). We mapped and analyzed individual macro- and meso-scale folds and associated faults in Miocene–Pliocene strata. Key horizons of light-colored quartz sandstone and carbonate rocks in the Palm Spring Formation provide structural markers, notably when restoring bed offsets and fault–fold geometries and kinematics. We address crosscutting relations of the Banning and Indio Hills faults with fold structures. Structural orientation data are obtained from meso-scale folds and faults and are integrated between the areal segments to link a prevalent pattern of deformation into a wider structural architecture (Fig. 2).

https://doi.org/10.5194/se-2022-9
Preprint. Discussion started: 2 February 2022

Results

Structural overview of the Indio Hills

The study area comprises three major SAFZ-oblique asymmetric, E–W-trending, moderately west-plunging fold systems with multiple smaller-scale parasitic folds (Fig. 2). The main folds affect most of the Palm Spring Formation in an approximately two kilometers wide zone between the-Banning and Indio Hills faults (Fig. 2). The northeastern flank of the Indio Hills is structurally different by consisting of a sub-horizontal, NW–SE-trending, open, upright anticline, which trends parallel to the Indio Hills fault (Fig. 2). Similarly, close to the Banning fault, tilted strata of the Palm Spring Formation are folded into a tight, steeply plunging shear fold (Fig. 2). At smaller scale, several subsidiary reverse faults and mostly right-slip, step-over faults with orientations both parallel with (E–W to NW–SE) and perpendicular (NNE–SSW) to the bounding faults exist within the macro-folded domain. Most of these faults truncate individual SAFZ-oblique folds.

SAFZ-oblique macro-folds

SAFZ-oblique macro-folds are consistently asymmetric and mostly south-verging, and their axial surfaces are arcuate and right-stepping in map view (Fig. 2). Fold geometries change from open and nearly upright near the Banning fault, via kink/chevron styles in the middle part, to very tight (isoclinal) and overturned fold styles adjacent to the Indio Hills fault (Fig. 3a–c). These changes in geometry correspond to a change in obliquity of the fold axial surface trace from approximately 60–70° to less than 20° with the Indio Hills fault (Fig. 2). All three macro-folds have axial trends that bend and partly merge into parallelism with the Indio Hills fault, whereas moderate to steeply WSW-dipping strata of the Palm Spring Formation are obliquely truncated by the Banning fault in the southwest. Tighter fold hinges are mapped in the central macro-fold and on the back-limb of the Z-shaped, southeastern macro-fold (Fig. 2).

Northwestern and central macro-folds

The northwestern and central macro-folds define two major, compound and arcuate fold systems that affect the entire Palm Spring Formation between the Banning and Indio Hills faults (Fig. 3a–b). They consist of eight subsidiary Z- and S-shaped, south-verging anticline-syncline pairs, and show fold axes plunging variably but mostly about 30° to the west (Fig. 2). At large scale, both folds tighten northeastward and display clockwise bend of axial traces from ENE–WSW near the Banning fault, to E–W and NW–SE when approaching the Indio Hills fault (Fig. 2 and 3c). Fold hinges in the west are typically symmetric,

https://doi.org/10.5194/se-2022-9
Preprint. Discussion started: 2 February 2022

concentric, and open (Supplement S1a–b), and become gradually tighter and dominantly Z-shaped kink folds eastward (Supplement S1c). The folds turn into tight, isoclinal, and inverted (Supplement S1d–e) when approaching the central macro-fold back-limb (Fig. 3b), and they potentially merge with the SAFZ-parallel anticline less than 200 meters from the Indio Hills fault (Fig. 2). A corresponding change in the geometry of the central macro-fold hinge zone is observed northeastward, i.e., from symmetric, via kink/chevron, to isoclinal overturned styles (Supplement S2a–b), until they flank the back-limb of the southeastern macro-fold (Supplement S2c–d). Bedding surfaces on the fore-limb of the central macro-fold dip steeply or are inverted, whereas strata on the back-limb mostly dip gently to the north or northwest, i.e., at a high angle to the bounding faults, and gradually change to northward dip when approaching the Indio Hills fault (Fig. 3c).

Another feature of the central macro-fold is that it is offset by a system of both layer-parallel and bed-truncating faults (Fig. 3b). Strata east of the fault system are affected by a large shear fold with thickened hinges and thinned limbs. The next fold to the north-northeast changes from open to tight, overturned, and locally isoclinal (Supplement S2a–c), and merges with the inverted, NE-dipping back-limb of the southeastern macro-fold (Fig. 3c). Notably, the consistent eastward tightening of fold hinges occurs within the lower stratigraphic units of the Palm Spring Formation, whereas the underlying Mecca Formation conglomerates are only weakly folded (see section about the southeastern macro-fold). Furthermore, beds in tighter folds are commonly accompanied by disharmonic folds and internal structural disconformities in relatively weak clayish–silty dark mudstone layers. On the contrary, more rigid, and thicker sandstone beds are more commonly fractured.

Southeastern macro-fold

The southeastern macro-fold is expressed as a kilometer-wide, Z-shaped, open to tight, south-verging syncline-anticline pair with moderately west-plunging axes and steeply north-dipping axial surfaces (Fig. 3c). Most of the Palm Spring Formation strata on the back-limb trend parallel to the Indio Hills fault and dip about 50–70° to the north, whereas strata in the hinge and fore-limb dip about 40–70° to the west/southwest (Fig. 3c). These attitudes combined with a relatively narrow hinge zone classify the southeastern macro-fold as a chevron type. The axial trend of the syncline-anticline pair is at a low angle (< 20°) to the Indio Hills fault but bends into a NE–SW trend westward with a much higher (oblique) angle to the Banning fault, which cuts off the fore-limb strata (Fig. 2). The southwestern macro-fold is very tight in the north and east and has several smaller-scale, tight to isoclinal, strongly attenuated folds on the main back-limb that merge from the central macro-fold, thus

https://doi.org/10.5194/se-2022-9
Preprint. Discussion started: 2 February 2022

indicating increasing strain intensity northeastward (see discussion). In contrast to the tightly folded beds of the Palm Spring Formation, bedding in the underlying Mecca Formation conglomerate is only weakly folded northeastward and becomes part of the open to monocline-like SAFZ-parallel anticline close to the Indio Hills fault.

A macro-folded siltstone layer of the lower Palm Spring Formation more than 200 meters southwest of the Indio Hills fault (Fig. 4a) contains centimeter-scale, upright (sub-horizontal) and disharmonic folds with E–W trend and western plunge (Fig. 4b). These intra-layer folded units are cut by low-angle reverse faults yielding a NE-directed sense-of-shear. The upright geometry and the sub-horizontal fold axes (about 5° plunge) of these intra-bed minor folds differ from the SAFZ-oblique folds but resemble those of the macro-scale, SAFZ-parallel NW–SE-trending anticline near the Indio Hills fault.

SAFZ-parallel macro-folds

About 100–200 meters southwest of the trace of the Indio Hills fault, the Mecca Formation conglomerate is folded into a major open anticline, whose axis is parallel to slightly oblique (< 20°) to the Indio Hills fault. This macro-fold is traceable with some confidence northwestward until the Indio Hills fault bends northward (Fig. 1). The southwestern limb of the fold marks the transition from the Mecca Formation conglomerate with the overlying Palm Spring Formation on the back-limb of the southeastern and central macro-folds (Fig. 2 and Supplement S2c). The conglomerate beds are thicker, almost unconsolidated, and much less internally deformed than the Palm Spring Formation strata. The major anticline displays an open, symmetric, partly box-shaped, NW–SE-trending, upright geometry with 2–3° plunge of the fold axis to the northwest. Outcrops on the SW-dipping limb of the anticline (Fig. 3c) are cut by a SW-dipping reverse fault system that is (sub-) parallel to the Indio Hills fault (Supplement S3a). These reverse faults may be linked with the reverse fault in folded strata of the Palm Spring Formation on the southeastern macro-fold back-limb described above (Fig. 4). The upright geometry and sub-horizontal NW–SE-trending axes of related small-scale folds in a mudstone layer (Fig. 4) resembles that of the SAFZ-parallel anticline.

A couple of major folds with axial traces parallel to the Banning fault is also well displayed on DEM images (Fig. 5). These folds affect WSW-dipping strata of the Palm Spring Formation on the broadened western part of the northwest and central macro-folds. The fold geometry is tight and asymmetric, with wavelengths less than 200 meters, and presumably steep NW-plunging axes. Its local appearance and sheared geometry contrast both

https://doi.org/10.5194/se-2022-9
Preprint. Discussion started: 2 February 2022

with the broad SAFZ-oblique folds near the Banning fault, and with that of the upright, SAFZ-parallel anticline near the Indio Hills fault.

Major and minor fold-related faults

Fold-related faults in the study area are mostly narrow damage zones less than one meter wide and are geometrically either related to SAFZ-oblique or SAFZ-parallel macro- and meso-scale folds, or are orthogonal to the SAFZ and related faults. Brittle faults exist both in granitic basement and in sedimentary rocks of the Mecca and Palm Spring formations. With exception of the main Banning and Indio Hills faults, brittle faults are generally difficult to trace laterally but are preserved in places with centimeter- to meter-scale strike-slip and/or reverse dip-slip offset. Large-scale fault orientations and kinematics in sedimentary rocks are more variable than in basement rocks, but strike commonly WNW–ESE to N–S and show moderate–steep dips to the northeast (Fig. 2). Subsidiary meso-scale faults include high-angle SW- and SE-dipping strike-slip faults, and low-angle SW-dipping thrust faults. We describe the Indio Hills and Banning faults, strike-slip faults, and thrust faults in sedimentary strata, and fractures in basement rocks northeast of the Indio Hills fault.

Indio Hills and Banning faults

Direct field observations of the strike and dip of the Indio Hills fault were not possible, but DEM images suggest a rectilinear geometry in map view relative to the uplifted strata (Fig. 2). The fault strikes mainly NW–SE and is subparallel to the northeastern flank of the Indio Hills. Farther southeast, it possibly merges with the Banning fault (Fig. 1; Tyler, 1974; Rymer, unpublished data). In the southeastern part of the study area (Fig. 2), the Indio Hills fault is most likely located between an outcrop of basement leuco-granite and the first outcrops of overlying strata of the Palm Spring Formation. The granite there is highly fractured and cut by vein and joint networks (see description below), as may be expected near a major brittle fault.

The Banning fault in the study area strikes WNW–ESE and is sub-vertical based on its consistent rectilinear surficial trace, and because it truncates both back- and fore-limb strata on most of the SAFZ-oblique macro-folds (Fig. 2). Thus, the Banning fault does not seem to have had major impact on the initial geometry and development of the macro-folds in the Indio Hills. However, notable exceptions include displacement of the two shear folds on the southern flank of the macro-folds by the Banning fault (Fig. 5), and a consistent anticlockwise bend of most axial traces of the macro-folds when approaching the Banning fault (Fig. 2).

https://doi.org/10.5194/se-2022-9
Preprint. Discussion started: 2 February 2022

Strike-slip faults in folded sedimentary strata

One major brittle fault set striking NW–SE and dipping steeply to the northeast has impact on the central macro-fold (Figs. 3b and 6). The faults splay out from a bedding-parallel core zone subparallel to steeply SW-dipping mud–silt-stone layers on the southern limb of the central macro-fold, and then proceed to truncate NW-dipping sedimentary strata and offset the hinge of a macro-fold by c. 70 meters right-laterally before dying out (Supplement S4a–b). The fault damage zone is traceable for more than one kilometer along strike as a right-slip fault which displaces the hinge of a major, tight, asymmetric, shear-like (similar style) fold (Fig. 6 and Supplement S5). The shear folded sedimentary strata bend clockwise toward the main fault, thus supporting dominant right-lateral slip (Fig. 6). Minor faults branch out from the fault core zone and either die out in the macro-fold hinge, and/or persist as bedding-parallel faults for some distance on the southern limb of the macro-fold (Fig. 6).

At smaller scale, the folded and tilted strata of the Palm Spring Formation are commonly truncated by sets of steep NW–SE-striking right-lateral and NNE–SSW-striking left-lateral faults, with meter- to centimeter-scale offsets (Supplement S4b–d). These minor faults generally dip steeply to the northeast to east-northeast, i.e., opposite to most bedding surfaces, which dip southwest (Fig. 3b), and, in places, develop reddish fault gouge along strike. Furthermore, these minor faults typically cut sandstone beds and flatten, and/or die out within, mudstone beds, which restricts their lateral extent to a few decimeters–meters. Kinematic indicators, such as offset of bedding surfaces and fold axial surfaces, yield mostly right-slip displacements, in places with minor reverse components. In some localities, on fold limbs within thick and competent sandstone beds, such minor right- and left-slip faults operate together defining conjugate sets (Supplement S4b and d) that may have formed simultaneously. In addition, NNE–SSW-striking, ESE-dipping faults and/or semi-brittle kink bands sub-orthogonal to the SAFZ are well displayed in the southeastern macro-fold (Fig. 3c and Supplement S4e) and cut bedding surfaces at high angles with left-slip displacement, therefore potentially representing cross faults between segments/splays of the SAFZ system.

Reverse faults in folded sedimentary strata

Reverse and thrust faults are common and traceable on the back-limb of the central and southeastern macro-folds near the SAFZ-parallel anticline and the Indio Hills fault, but not recorded in areas close to the Banning fault. Reverse faults strike mainly NW–SE and dip gently to the southwest, although subsidiary gently NE-dipping faults exist. An example is the low-angle reverse fault that propagates out-of-the syncline on the southeastern macro-fold (Fig. 4) and yields a NE-directed sense-of-shear. This thrust fault may continue westward into the central macro-fold (Fig. 3b), where reverse offset of SW-dipping strata of the Palm Spring Formation constrains vertical displacement from about 10–15 meters (Supplement S3a), though offset is only of a few centimeters in the southeast (Fig. 4). This fault system has a listric geometry, and internal splay faults die out in thick silt- to mud-stone layers. The low-angle faults seem to develop almost consistently near major fold hinge zones and propagate northeastward as out-of-the syncline thrusts (Fig. 4 and Supplement S3a).

In sandstone beds on the north-dipping limb of the major syncline, minor scale thrust faults, offset asymmetric fold hinges (Supplement S4c) and yield down-to-the-north (normal) sense of shear if the strata are restored to a horizontal position (Supplement S6). An opposite effect is apparent for a conjugate set of minor normal faults in a small-scale graben structure on the steep, north-dipping layer, which defines a set of reverse faults when restoring the sedimentary strata to horizontal (Supplements S4d and S6).

Fractures and faults in basement rocks north of the Indio Hills fault

Basement rock exposures in the Indio Hills are limited to a single, approximately 50 meters long chain of outcrops located in the southeasternmost part of the study area (Fig. 2). These outcrops of massive granite are heavily fractured with mostly steep to sub-vertical sets that strike dominantly NE–SW to ENE–WSW and subsidiary NW–SE to NNW–SSE, possibly representing, conjugate sets. Kinematic indicators are generally lacking, but in highly fractured areas, centimeter-thick lenses of unconsolidated reddish gouge are present, comparable to fault rocks observed in Palm Spring Formation sedimentary rocks and corresponding to similar small-scale strike-slip and reverse faults in the basement granite.

Discussion

Evolution of SAFZ-oblique folds

Three macro-scale fold systems are mapped and analyzed in between the Indio Hills and Banning faults. The folds are arranged in a right-stepping, and increasingly asymmetric (Z-shaped), and sigmoidal northeastward (Fig. 2). Thus, we classify them as modified SAFZ-oblique *en echelon* macro-folds. Similar fold geometries in sedimentary strata are described from many other segments of the SAFZ and formed by right-lateral displacement between two major fault strands due to distributed, right-lateral simple shear (Babcock, 1974; Miller, 1998; Titus et al., 2007; Bergh et al., 2019). The present fold orientation data, however (Fig. 2), do not correspond with a uniform simple shear model because the long axis of the strain ellipse is not about 45° to the shear zone as expected (Sanderson and Marchini, 1984; Sylvester, 1988). Instead, fold geometries vary both across and along strike, e.g., axial surface

https://doi.org/10.5194/se-2022-9
Preprint. Discussion started: 2 February 2022

traces of dying-out macro-fold hinges are at high obliquity angles (> 50–65°) near the Banning fault, whereas they are at much lower angles (< 20–30°) and merge with sigmoidal-shaped patterns against the Indio Hills fault (Fig. 2). Thus, we propose that the SAFZ-oblique macro-folds in Indio Hills evolved from boundary faults being active progressively through time. For example, a model in which the folds initially splayed out from an early active Indio Hills fault through right-lateral distributed displacement (e.g., Titus et al., 2007) is consistent with fold hinges extending outward south of the Indio Hills fault and dying out (broadening) away from the fault in a one–two kilometer-wide damage zone (Fig. 2). Furthermore, the initial upright, *en echelon* folding clearly occurred after deposition of the entire Palm Spring Formation, thus favoring folds propagating outward from the Indio Hills fault. By contrast, the Banning fault truncates both limbs of the open-style, *en echelon* folds (Fig. 2), which therefore indicates a younger slip event.

The moderate–steep westward plunge of all three macro-folds (≥ 30°), however, shows that the presumed initial horizontal fold hinges rotated into a steeper plunge. Such steepening may be due to, e.g., progressive shortening strain above a deep-seated fault, a hidden splay of the Indio Hills fault, or to an evolving stage of distributed shortening (folding) adjacent to the master strike-slip faults (e.g., Bergh et al., 2019), with gradually changing stress–strain orientation through time. This kind of fold reworking favors a situation where the northwestern and central macro-folds were pushed up and sideways (right-laterally), following the topography and geometry of an evolving convergent tectonic wedge. The corresponding eastward tightening, enhanced shear folding, and recurrent SW-directed overturned geometries of the central macro-fold on the back-limb of the southeastern macro-fold near the Indio Hills fault (Fig. 3b) support this idea. We propose a progressive model that changes from distributed (*en echelon* folding) to partly partitioned, i.e., pure shear (shortening) plus simple shear (strike-slip) deformation, as inferred for parts of the SAFZ, e.g., in the Mecca Hills (Bergh et al., 2019). In this model, the tight –to isoclinal fold geometries to the northeast (Fig. 3b) may account for progressively more intense shortening near the Indio Hills fault, whereas coeval strike-slip faulting affected the already folded and steeply dipping strata of the lower Palm Spring Formation (Fig. 6). This model would favor shortening strain to have evolved synchronously with renewed strike-slip shearing adjacent to the Indio Hills fault, and/or on a hidden fault below the contact between the Palm Spring and Mecca formations, because the Mecca Formation is much less deformed (Fig. 3c). Alternatively, the more mildly deformed character of the Mecca Formation conglomerate may arise from its homogeneity, which contrasts with alternating successions of mudstone–

https://doi.org/10.5194/se-2022-9
Preprint. Discussion started: 2 February 2022

siltstone and sandstone of the Palm Springs Formation prone to accommodating large amounts of deformation and to strain partitioning. Regardless, such reshaping of *en echelon* folds is supported by analog modelling (McClay et al., 2004; Leever et al., 2011a, 2011b) suggesting that partly partitioned strain may lead to a narrowing of fold systems near a major strike-slip fault (i.e., Indio Hills fault), whereas widening away from the fault indicates still ongoing distributed deformation (i.e., near the Banning fault). Partly partitioned deformation is supported by the tight to isoclinal and consistent Z-like geometry of smaller-scale folds present on the back-limb of the central and southeastern macro-folds (Fig. 3b–c), indicating that they are all parasitic folds and related to the same partly partitioned shear-folding event. Where S- and Z-like fold geometries are present, these minor folds may have formed by buckling in an early stage of *en echelon* folding. An alternative interpretation is that the tight, reshaped parasitic folds are temporally linked to the SAFZ-parallel macro-fold south of the Indio Hills fault (Fig. 3c; see next section).

Evolution of SAFZ-parallel folds

The SAFZ-parallel anticline differs significantly in geometry from the *en echelon* macro-folds and associated parasitic folds by having an upright and symmetric geometry < 20° oblique to the Indio Hills fault (Fig. 3c). Thus, it resembles that of a dip-slip fault-parallel fold in a more advanced partitioned transpressional segment of the SAFZ (e.g., Titus et al., 2007; Bergh et al., 2019). We suggest that this fold formed by dominant NE–-SW-oriented horizontal shortening, i.e., at high obliquity to the main Indio Hills fault (near-orthogonal pure shear), and/or as a fault-related fold above a buried, major reverse oblique-slip splay of the Indio Hills fault at depth (e.g., Schlische, 1995). The timing might be after the tight reworking of *en echelon* folds, i.e., comparable to other settings (e.g., western Svalbard; Bergh et al., 1997; Braathen et al, 1999). The idea of a late-stage, highly oblique pure-shear overprint onto the macro-folds is supported by small-scale upright folds located within the tight *en echelon* syncline on the back-limb of the modified central macro-fold system (Fig. 4). The NW–SE trend, upright style, and negligible plunge of the fold axes indicate that these folds may be superimposed on the steeper plunging and reshaped *en echelon* folds, and/or that they formed in progression to an increased component of NE–SW shortening on the Indio Hills fault. Nonetheless, it is possible that these folds formed simultaneously with the *en echelon* macro-folds due to uncertain crosscutting relationships.

Progressive NE–SW-oriented contraction may have triggered formation of the upright SAFZ-parallel anticline adjacent to the Indio Hills fault (Fig. 2), which then acted as a SW-

https://doi.org/10.5194/se-2022-9
Preprint. Discussion started: 2 February 2022

dipping thrust fault with top-NE displacement. The oblique shortening then led to a certain amount of uplift near the Indio Hills fault, and possibly also accomplished the overturning of folds on the northeastern back-limb of the central and southeastern macro-fold. A similar mode of advanced partitioned shortening was proposed for SAFZ-parallel fold structures in central and southern California (Mount and Suppe, 1987; Titus et al., 2007; Bergh et al., 2019). Our results are supported by stress orientation data acquired by Hardebeck and Hauksson (1999) along a NE–SW-trending profile across the Indio Hills. They recorded an abrupt change in the maximum horizontal stress direction from about 40° oblique to the SAFZ around the Banning fault, to about 70° oblique (i.e., sub-orthogonal) farther northeast, near the Indio Hills fault, which supports the change in attitude and shape of macro-fold geometries that we have outlined. Shortening and strike-slip partitioning, however, would require synchronous right slip on another major fault strand, e.g., the Banning fault, a hypothesis that is supported by the recorded late shear folding there (Fig. 5).

Fault interaction, evolution, and relative timing

Prior to inversion and uplift of the Indio Hills, the Indio Hills fault most likely acted as a SW-dipping, extensional, basin-bounding normal fault. Evidence of an early-stage episode of extension is preserved as micro-fault grabens in steeply dipping layers (Supplements S3b and S6). Alternatively, the Indio Hills fault dips northeast and uplifted the granitic basement rocks in the hanging wall to the northeast, followed by erosion of the overlying Mecca, Palm Spring and Ocotillo formations there (Fig. 1). We favor a steep, SW-dipping normal fault that was progressively reactivated as an oblique-slip reverse/thrust fault.

Right-lateral to right-lateral-reverse movement along the Indio Hills fault that led to the formation of the SAFZ-oblique *en echelon* macro-folds also indicates a steeply dipping character for the precursory Indio Hills fault, which gradually changed to a dominantly right-lateral-reverse fault. The change to a right-lateral-reverse fault is supported by the presence of both meso-scale strike-slip and thrust faults with similar NW–SE strikes (Fig. 4, and Supplements S2c and 3a). The increased reverse component of faulting may have triggered rotation of the *en echelon* macro-fold axes to a steeper plunge, reshaped the open asymmetric folds into tight overturned folds, and caused gentle buckling of strata in the nearby SAFZ-parallel anticline. Hence, the Indio Hills fault acted as an oblique-slip thrust oblique to the margin, which is supported by oblique maximum horizontal stress near the Indio Hills fault (c. 70°; Hardebeck and Hauksson, 1999), while the Banning fault accommodated right slip.

https://doi.org/10.5194/se-2022-9
Preprint. Discussion started: 2 February 2022

By contrast, the last slip event on the Banning fault is clearly younger than the episode of *en echelon* folding, from its truncating attitude (Fig. 2). However, the anticlockwise bending of the axial traces into an ENE–WSW trend when approaching the Banning fault suggests that a distributed component of stress also affected the area around the fault in its early kinematic stages. The refolding of the southwest limb of the central macro-fold near the Banning fault (Fig. 5) also favors a late-stage activation of this fault.

Minor faults in the Indio Hills provide additional input to resolve the spatial and temporal relations between macro-fold and fault interaction in the Indio Hills. We analyzed minor fault-related folds (Supplement S3c), which, in their current position on steep north-dipping beds, define down-to-the north displacement, but define a low-angle fold and thrust system when restored to horizontal (Supplement S6). These geometric relationships suggest that the minor folds and faults pre-date (or were coeval with) the SAFZ-oblique macro-folding event, and that they formed initially as internal fractures due to N–S-oriented shortening when the sedimentary strata were still horizontal, i.e., that some partitioning (e.g., SAFZ-parallel small-scale thrust faults) occurred simultaneously with distributed deformation (e.g., SAFZ-oblique *en echelon* macro-folds).

Further, our field data suggest that minor right-slip faults evolved synchronously and parallel with the E–W-trending *en echelon* fold limbs, propagating through rheologically weaker mudstone beds that flowed plastically and acted as slip surfaces during distributed deformation. Later or simultaneously, these faults propagated beyond the mudstone beds as NW–SE-striking right-slip faults adjacent to tightened shear folds during partly partitioned deformation, and finally ended up with truncation of the SAFZ-oblique folds (Fig. 6 and Supplement S4a–c).

The presence of out-of-the syncline reverse/thrust faults relative to the reshaped and tightened SAFZ-oblique macro-folds (Fig. 4 and Supplement S3a and d) where SW-dipping thrust faults formed (sub-) parallel to the Indio Hills fault and the related anticline (Fig. 3c) suggests successive distributed and partly partitioned strain in the study area. The proximity and superimposed nature of reverse/thrust faults relative to the reshaped *en echelon* folds suggest that they utilized modified fold hinges and steeply tilted limbs as preexisting zones of weakness. Despite the uncertainty around the crosscutting relationship between the SAFZ-parallel anticline and the SAFZ-oblique *en echelon* macro-folds, the layer-parallel thrust and intra-detachment folds in the southeastern macro-fold (Fig. 4) indicate that such thrust detachments may have already formed during (early?) distributed deformation, i.e., that distributed and partitioned deformation occurred simultaneously and/or progressively.

https://doi.org/10.5194/se-2022-9
Preprint. Discussion started: 2 February 2022

The conjugate WNW–ESE- to NNW–SSE-striking right-slip and NNE–SSW-striking left-slip faults and kink band features truncate strata on both macro-fold limbs (Fig. 3b–c) with an acute angle perpendicular to the macro-folded and tilted Palm Spring Formation strata (e.g., Supplement S4e). Thus, they formed together with or after the *en echelon* macro-folding.

Tectonic model

Our field and structural data support inversion and uplift of the Indio Hills involving progressive or stepwise stages of folding and faulting events with a switch from distributed to partly partitioned transpression (Fig. 7). Prior to inversion in Miocene time, the Indio Hills fault may have been a steep, SW-dipping normal fault that bounded granitic basement rocks in its footwall to the northeast. These basement rocks were partly eroded and overlain by the Mecca Formation, most likely at 4.0–3.7 Ma, and by the succeeding, lower and upper Palm Spring Formation strata respectively at 3.7–2.8 Ma and 2.8–1.0 Ma, as suggested from paleomagnetic studies in the Mecca Hills (McNabb et al., 2017).

Early inversion involved distributed transpressional strain triggered by right-lateral slip along the Indio Hills fault (Fig. 7a). Three macro-scale, upright *en echelon* folds and associated parasitic folds formed in loosely consolidated sedimentary rocks of the Mecca and Palm Spring formations. These SAFZ-oblique folds displayed a right stepping pattern with E–W-trending axial surfaces, probably at a high angle (45º) to the bounding master fault(s) due to uniform simple shear (e.g., Sanderson and Marchini, 1984; Sylvester, 1988). This is notably observed in the less deformed southwestern part of the study area (Fig. 2) near the precursory Banning fault. Bed-internal minor fold and fault systems in weak mudstone beds (Fig. 4 and Supplement S3a) may have formed parallel to the E–W-trending *en echelon* fold traces, either as thrust detachments due to oblique N–S shortening when strata were horizontal, and/or as strike-slip faults on the fold limbs. In addition, minor (bed-internal) SAFZ-parallel thrusts and folds formed prior to or together with the *en echelon* macro-folds (Supplements S2b–c and 6a–b), thus suggesting minor partitioning.

Further deformation led to gradual change to partly partitioned shortening and right-lateral faulting and folding (Fig. 7b), probably since the Indio Hills fault started to accommodate an increasing amount of reverse slip, thus acting as an oblique-slip reverse fault, and where the Banning fault seems to have still played a minor role. The main result was attenuation of the macro-folds toward the Indio Hills fault, increased shear folding, and clockwise rotation of fold axes to a steeper westerly plunge, whereas buckle-folding

https://doi.org/10.5194/se-2022-9
Preprint. Discussion started: 2 February 2022

continued in the southwest (Fig. 7b). Increased shortening and shearing reshaped the macro-folds and their back-limb folds to tight, isoclinal, and partly overturned folds with consistent Z-style and sigmoidal axial-surface traces near the Indio Hills fault (Fig. 7b). The sigmoidal pattern of the WNW–ESE-trending *en echelon* macro-folds formed at a much lower angle with the Indio Hills fault (< 20–30°) than with the Banning fault (60–70^0). The incremental component of lateral strain is recorded as progressively crosscutting NW–SE-striking, strike-slip shear faults terminating with local truncation of the central macro-fold (see Fig. 7c and section below).

Late-stage uplift was marked by a gradual switch to more evolved transpressional strain partitioning, where the dominant shortening component affected the Indio Hills fault as a right-lateral-oblique thrust fault and the main strike-slip component was centered along the Banning fault (Fig. 7c). NE-directed oblique thrusting on the Indio Hills fault and related minor, reverse, out-of-the syncline faults led to uplift, which resulted in formation of a major anticline parallel to the Indio Hills fault in sediments of the Mecca Formation (Fig. 7c). With increasing partitioning, margin-parallel slip was accommodated by right-slip along the linear Banning fault, where subvertical folds formed locally, and presumed antithetic conjugate kink band sets of right- and left-slip cross faults affected the entire uplifted area.

We favor a progressive evolution from distributed to partly partitioned deformation as presented in Fig. 7a–c, although overlapping and synchronous formation of various structures may have occurred, at least locally (except for the late-stage Banning fault and related shear folds). The latter is based on uncertainties in our field data, e.g., variable cross-cutting relations of early, bedding-parallel strike-slip and thrust faults and *en echelon* macro-folds (Figs. 4 and 6, and Supplements S3c–d and S4), and from the spatial variations in the direction of maximum horizontal stress across the Indio Hills at present, from 40° oblique to the boundary faults near the Banning fault to 70° oblique near the Indio Hills fault (Hardebeck and Hauksson, 1999).

The present model and right-lateral-reverse character of the Indio Hills fault are further supported by the relationship of the Indio Hills fault with the East California Shear Zone, which merge together north of the study area where the Indio Hills fault bends into a NNW–SSE strike along the Landers–Mojave Line (Dokka and Travis, 1990a, 1990b; Thatcher et al., 2016). Recent activity along the Landers–Mojave Line recorded as six–seven earthquakes with M > 5 between 1947 and 1999 (Fig. 1; Nur et al., 1993a, 1993b; Du and Aydin, 1996; Spinler et al., 2010) indicates that the Indio Hills fault may transfer

https://doi.org/10.5194/se-2022-9
Preprint. Discussion started: 2 February 2022

displacement from unsuitably oriented right-slip faults in the north, such as the Calico and Camp Rock faults, to the main SAFZ strand (Fig. 1).

Farther southeast along strike, the Indio Hills and Banning faults merged along a dextral freeway junction (Platt and Passchier, 2016) that may have enhanced, wedge-shaped transpressional uplift of the Indio Hills after the (late) formation of the Banning fault (Fig. 8a–c). However, anticlockwise rotation of the Indio Hills block and related structures in map view as predicted in a dextral freeway junction (Platt and Passchier, 2016) was not recorded by our field data (except along the Banning fault due to localized right-slip along the fault; cf. sub-vertical shear fold in Fig. 5). This may be due in part to the late formation of the Banning fault (< 1 Ma), i.e., clockwise rotation (in map view) of the fold and fault structures due to right-lateral slip along the Indio Hills fault, and to the oblique-slip character of the Indio Hills fault. Thus, the dextral freeway junction in the Indio Hills may be more of a transitional nature. Instead of major anticlockwise rotation of the Indio Hills block in map view, the accretion of material toward the fault junction due to right slip along the Banning fault is probably partly accommodated by the dominant vertical slip component along the Indio Hills fault, leading to further uplift near the junction (i.e., clockwise rotation in cross section).

Regional comparison and implications

The proposed progressive tectonic model for the Indio Hills uplift has wide implications when compared and correlated with other fault strands of the SAFZ bounding uplifted domains along strike in the Coachella and Imperial Valleys (Fig. 8), and in explaining lateral variations in fault architectures, kinematic evolution and timing, deformation mechanisms and areal segmentation (Sylvester and Smith 1987; McNabb et al., 2017; Janecke et al., 2018; Bergh et al., 2019).

Comparison with the Mecca Hills

Previous studies of SAFZ-related uplifts between the Indio Hills and Durmid Hills in Coachella Valley show that the Indio Hills and Banning faults link up directly with the main SAFZ strand in the Mecca Hills (Fig. 8c) which then, together with the subsidiary Skeleton Canyon and Painted Canyon faults, bounds a much wider flower-like uplift area than in the Indio Hills (Fig. 8c; Sylvester and Smith, 1976, 1987; Sylvester, 1988; McNabb et al., 2017; Bergh et al., 2019). In contrast to the Indio Hills fault, however, the main SAFZ in Mecca Hills has an anastomosing geometry with thick (10–500 m), red-stained fault gouge. Regardless, we consider them to be correlative and infer the lack of fault gouge in Indio Hills fault to be due to more localized strain on the Indio Hills fault than on the SAFZ in Mecca

Hills. This is supported by a more rectilinear geometry and lack of fold–fault linkage in Indio Hills, which may have allowed initial lubrication of the fault surface in basement rocks with high contrasting rheology (e.g., Di Toro et al., 2011; Fagereng and Beall, 2021), and which hampered fluid circulation and extensive cataclasis.

Both the Indio Hills and Mecca Hills uplift areas are bounded to the northeast by a presumed Miocene, SW-dipping normal fault (Fig. 8a), which later acted as major SAFZ-parallel oblique-reverse faults, and which significantly contributed to the uplift of these areas in Pliocene–Pleistocene time (Sylvester and Smith, 1976, 1987; McNabb et al., 2017; Bergh et al., 2019). In the Mecca Hills (Fig. 8c), the Painted Canyon fault is flanked in the hanging-wall to the southwest by a basement-cored, macro-fold (Mecca anticline), which is similar to the upright anticline that parallels the Indio Hills fault and adjacent minor thrust faults (**Error! Reference source not found.**). Similar folds appear adjacent to the Hidden Springs–Grotto Hills fault (Sheridan et al., 1994; Nicholson et al., 2010), a NW–SE-striking, now reverse splay fault of the main SAFZ between the Mecca Hills and Durmid Hills (Fig. 8c). It is, however, unlikely that these marginal faults link up directly along strike. Rather, they merge or splay with the SAFZ and SAFZ-oblique faults.

The inversion and main uplift history of the Mecca Hills segment of the SAFZ (Bergh et al., 2019) initiated with right-lateral slip on a steep SAFZ, from where SAFZ-oblique *en echelon* folds and dominantly right-slip faults splayed out in a one–two kilometers wide damage zone on either side of the SAFZ (Fig. 8a). The subsidiary Skeleton Canyon fault initiated as a steep right-lateral and SAFZ-parallel strike-slip fault along a small restraining bend (Fig. 8b). Successive lateral shearing reshaped the *en echelon* folds into steeply plunging folds with axial traces parallel to the SAFZ. The final kinematic stage generated SW-verging fold and thrust structures parallel to the SAFZ (Fig. 8c), which truncated the *en echelon* folds and the NE-dipping Skeleton Canyon fault. The resulting wedge-like flower structure thus records a polyphase kinematic evolution from distributed, through locally partitioned, to fully partitioned strain in a changing transpressional plate regime (Bergh et al., 2019).

Based on the geometric similarities, we consider that the *en echelon* macro-folds in both Indio Hills and Mecca Hills formed simultaneously, but not on the same regional fault strand (Fig. 8a). In both areas, the *en echelon* folds and faults are strongly reworked and tightened into sigmoidal shapes where they merge with the Indio Hills and Skeleton Canyon faults respectively (Fig. 8b; Bergh et al., 2019), and SAFZ-parallel thrust faults formed early (i.e., prior to macro-folding) both in the Indio Hills (Supplement S3c–d) and in the Mecca Hills (Rymer, 1994), thus supporting continuous partly partitioned strain field in both areas.

https://doi.org/10.5194/se-2022-9
Preprint. Discussion started: 2 February 2022

Strain partitioning caused major uplift of the Mecca Hills block along the Skeleton Canyon, Painted Canyon, and Hidden Springs–Grotto Hills faults (Fig. 8c), all acting as SAFZ-parallel oblique-slip thrust faults (Sheridan et al., 1994; Bergh et al., 2019). The partitioned right-slip component was partly transferred to the Banning fault in Indio Hills, and/or to an unknown hidden fault southwest of the SAFZ (e.g., in Mecca Hills; Hernandez Flores, 2015; Fuis et al., 2017), possibly the Eastern Shore line fault (Janecke et al., 2018).

Based on paleomagnetic and structural field studies, uplift of the SAFZ-related Mecca basin started at ca. 3.0–2.2 Ma and culminated at 1.0–0.76 Ma, i.e., after deposition of the Palm Spring Formation (McNabb et al., 2017; Janecke et al., 2018). Uplift is still ongoing at present (Fattaruso et al., 2014; Janecke et al., 2019). A comparable time frame and ongoing activity are expected for the Indio Hills.

Comparison with Durmid Hills

The Durmid ladder structure along the southern 30 kilometers of the SAFZ in Imperial Valley defines a similar but oppositely merging, one–three kilometers wide wedge-shaped uplift as in Indio Hills, bounded by the right-lateral and reverse Eastern Shore fault to the southwest and the main SAFZ to the northeast (Fig. 8c; Janecke et al., 2018). Internally, the ladder structure comprises *en echelon* folds (Babcock, 1974; Bürgmann, 1991) that merge in a sigmoidal pattern with the main SAF, and subsidiary sets of conjugate SAFZ-parallel right-lateral and SAFZ-oblique E–W-striking, left-slip cross faults, which accommodated clockwise rotation of internal blocks (Janecke et al., 2018). By assuming a northwest continuation of the main SAFZ with the SAFZ in Mecca Hills, the Eastern Shore fault has no exposed correlative fault in the Mecca Hills and Indio Hills (Fig. 8c; Damte, 1997; Bergh et al., 2019). Nevertheless, the Eastern Shore fault may continue at depth southwest of the Banning fault and main SAFZ (Janecke et al., 2018).

The increasing width of damage zones adjacent to SAFZ-related faults southward in Coachella Valley, and increased number of strike-slip and oblique to orthogonal cross faults in the Durmid Hills compared with Indio Hills and Mecca Hills may be due to closeness and transition to a transtensional rift setting around the Brawley seismic zone (Janecke et al., 2018). A significant difference between the Indio Hills–Mecca Hills and the Durmid Hills, however, is the large number of cross faults in the Durmid ladder structure. Such faults are interpreted as early-stage, NE–SW-striking, left-lateral, faults (Fig. 8a), which were rotated clockwise by progressive right-lateral motion into sigmoidal parallelism with the SAFZ and Eastern Shoreline fault (Fig. 8b–c; Janecke et al. 2018). In contrast, cross faults in Indio Hills are much less common and, where present, possibly formed late, but prior to the Banning

https://doi.org/10.5194/se-2022-9
Preprint. Discussion started: 2 February 2022

fault. Thus, in the Indio Hills, there is no evidence of clockwise rotation of early-stage cross faults as in the Durmid Hills, but rather clockwise rotation of fold axial traces is common, which may be a first step in the formation of ladder-like fault blocks (e.g., Davis, 1999; Schultz and Balasko, 2003).

A major outcome of the comparison with Durmid Hills is that the wedge-shaped uplift block between the Indio Hills and Banning faults may represent a failed uplift and/or the early stage of formation of a ladder structure. This idea is supported by presence of similar master faults and structures with comparable kinematics in both the Indio Hills and Durmid Hills, including oblique *en echelon* macro-folds, strike-slip faults acting as step-over faults, and reverse faults. Younger, non-rotated, conjugate cross faults exist in the Indio Hills but not in the Durmid Hills where such faults are more evolved features due to larger strain and more advanced stage of ladder structure formation. From these observations, one should expect to find ladder structures operating at different evolution stages among the many, yet unexplored uplifts in Coachella Valley.

Conclusions

1) The Indio Hills segment of the SAFZ in Coachella Valley, southern California evolved as a wedge-shaped uplift block between two major SAFZ-related fault strands, the Indio Hills and Banning faults, which merge in a dextral freeway junction of a transitional nature to the southeast.
2) The Indio Hills fault acted as a SW-dipping, basement-seated normal fault in Miocene time, i.e., prior to inversion as an oblique-slip, right-lateral-reverse fault during Pliocene and Pleistocene times, whereas the Banning fault initiated probably during the later stages of uplift as a dominantly right-slip fault.
3) Transpressive deformation triggered uplift and inversion of the Indio Hills through a progressive change from distributed *en echelon* folding to partly partitioned right-slip thrusting. We favor a progressive rather than stepwise model in which the main uplift was related to late shortening in at the freeway junction where the Indio Hills and Banning faults merge.
4) The Indio Hills fault is a splay fault of the SAFZ that merges to the north with the Landers–Mojave Line and transfers slip from unsuitably oriented faults of the Eastern California Shear Zone to the Banning fault portion of the SAFZ in the southeast.
5) A significant difference of the Indio Hills with the Durmid Hills is that left-lateral step-over and cross faults in the Durmid Hills rotated subparallel with the mSAF,

whereas in Indio Hills, all cross faults are oblique with the SAFZ and, thus, may reflect an earlier stage of a still evolving ladder structure.

Data availability

The structural dataset and field photographs used in the present study are available on DataverseNO (Open Access repository) at https://doi.org/10.18710/TM18UZ. DEM images are from Google Earth (© Google Earth 2011).

Authors contribution

All authors contributed to collect structural measurements in the Indio Hills. JBPK wrote the first draft of the manuscript and designed half the figures and supplements (workload: 35%). Prof. SGB made major revision to the initial draft and designed half the figures and supplements (workload: 35%). Prof. AGS also revised the manuscript and provided major input about the local geology (workload: 30%).

Competing interests

The authors declare that they have no known competing interests.

Acknowledgments

The staff at the University of California–Santa Barbara and San Diego State University provided great hospitality during Steffen Bergh's sabbatical leaves in 2011–2012 and 2016–2017 while working with the San Andreas fault. We thank all the persons from these institutions that were involved in this project. The authors thank Prof. Emeritus Arild Andresen (University of Oslo) and Prof. Holger Stunitz (UiT) for helpful comments and Jack Brown (San Diego State University) for fieldwork collaboration. Prof. Susanne Janecke (Utah State University) and Dr. Miles Kenney (Kenney Geoscience) provided fruitful discussion.

Financial support

The present study is part of the CEED (Centre for Earth Evolution and Dynamics) and ARCEx projects (Research Centre for Arctic Petroleum Exploration), which are funded by grants from UiT The Arctic University of Norway in Tromsø and the Research Council of Norway (grant numbers 223272 and 228107) together with eight academic and six industry partners.

Solid Earth Discussions

References

Allen, C. R.: San Andreas fault zone in San Gorgonio Pass, southern California, GSA Bull., 68, 315–360, 1957.

Atwater, T. and Stock, J.: Pacific-North America Plate Tectonics of the Neogene Southwestern United States: An Update, International Geology Review, 40:5, 375–402, 1998.

Babcock, E. A.: Structural Geology and Geophysics of the Durmid Area, Imperial Valley, California, Ph.D. Thesis, University of California, Riverside, 149 pp., 1969.

Babcock, E. A.: Geology of the northeast margin of the Salton Trough, Salton Sea, California, GSA Bull., 85, 321–332, 1974.

Bergh, S. G., Braathen, A. and Andresen, A.: Interaction of basement-involved and thin-skinned tectonism in the tertiary fold-and thrust belt of Central Spitsbergen, Svalbard, AAPG Bull., 81, 637–661, 1997.

Bergh S. G., Sylvester, A. G., Damte, A. and Indrevær, K.: Evolving transpressional strain fields along the San Andreas fault in southern California: implications for fault branching, fault dip segmentation and strain partitioning, Geophys. Res. Abs., 16, EGU General Assembly, 24th April–2nd May, Vienna, Austria, 2014.

Bergh, S. G., Sylvester, A. G., Damte, A. and Indrevær, K.: Polyphase kinematic history of transpression along the Mecca Hills segment of the San Andreas fault, southern California, Geosphere, 15, 34 pp., 2019.

Bilham, R. and Williams, P.: Sawtooth segmentation and deformation processes on the southern San Andreas fault, California, Geophys. Res. Lett., 12, 9, 557–560, 1985.

Blisniuk, K., Scharer, K., Sharp, W. D., Burgmann, R., Amos, C. and Rymer, M.: A revised position for the primary strand of the Pleistocene-Holocene San Andreas fault in southern California, Sci. Adv., 7, eaaz5691, 2021.

Boley, J.-L., Stimac, J. P., Weldon II, R. J. and Rymer, M. J.: Stratigraphy and paleomagnetism of the Mecca and Indio Hills, southern California, in: Geological Investigations of an Active Margin, edited by: McGill, S. F. and Ross, T. M., GSA, Cordilleran Section Guidebook, 27th Annual Meeting, San Bernardino County Museum Associations, USA, 336–344, 1994.

Braathen, A., Bergh, S. G. and Maher Jr., H. D.: Application of a critical wedge taper model to the Tertiary transpressional fold-and thrust belt on Spitsbergen, Svalbard, GSA Bull., 111, 1468–1485, 1999.

https://doi.org/10.5194/se-2022-9
Preprint. Discussion started: 2 February 2022

Bürgmann, R.: Transpression along the southern San Andreas fault, Durmid Hills, California, Tectonics, 10, 1152–1163, 1991.

Chang, S.-B. R., Allen, C. R. and Kirschvink, J. L.: Magnetic stratigraphy and a test for block rotation of sedimentary rocks within the San Andreas fault zone, Mecca Hills, southeastern California, Quat. Res., 27, 30–40, 1987.

Dair, L. and Cooke, M. L.: San Andreas fault geometry through the San Gorgonio Pass, California, Geology, 37, 2, 119–122, 2009.

Damte, A.: Styles of deformation in zones of oblique convergence: Examples from the Mecca Hills, southern San Andreas fault, Unpublished Ph.D. thesis, University of California, Santa Barbara, 164 pp., 1997.

Davis, G. H.: Structural geology of the Colorado Plateau region of southern Utah, with emphasis on deformation bands, GSA Spec. Pap., 342, 157 pp., 1999.

Di Toro, G., Han, R., Hirose, T., De Paola, N., Nielsen, S., Mizoguchi, K., Ferri, F., Cocco, M. and Shimamoto, T.: Fault lubrication during earthquakes, Nature, 471, 494–498, 2011.

Dibblee, T. W. Jr.: Geology of the Imperial Valley, California, Californian Division of Mines Bulletin, 170, 21–28, 1954.

Dibblee, T. W. Jr.: Geology of the southeastern San Andreas fault zone in the Coachella Valley area, Southern California, in: Southern San Andreas fault, Whitewater to Bombay Beach, Salton Trough, California, edited by: Baldwin, J., Lewis, L., Payne, M. and Rocquemore, G., South Coast Geological Society, Annual Field Trip Guide Book, 25, 35–56, 1997.

Dibblee, T. W. Jr. and Minch, J. A.: Geological map of the Thousand Palms & Lost Horse Mountain 15 minutes quadrangles, Riverside County, California, Dibblee Foundation, Map DF-372, 2008.

Dokka, R. K. and Travis, C. J.: Late Cenozoic strike-slip faulting in the Mojave Desert, California, Tectonics, 9, 311–340, 1990a.

Dokka, R. K. and Travis, C. J.: Role of the Eastern California Shear Zone in accommodating Pacific-North American plate motion, Geophys. Res. Lett., 17, 1323–1326, 1990b.

Dorsey, R. J., Housen, B. A., Janecke, S. U., Fanning, C. M. and Spears, A. L. F.: Stratigraphic record of basin development within the San Andreas fault system: Late Cenozoic Fish Creek–Vallecito basin, southern California, GSA Bull., 123, 5/6, 771–793, 2011.

https://doi.org/10.5194/se-2022-9
Preprint. Discussion started: 2 February 2022

Du, Y. and Aydin, A.: Is the San Andreas big bend responsible for the Landers earthquake and the eastern California shear zone, Geology, 24, 3, 219–222, 1996.

Fagereng, Å. and Beall, A.: Is complex fault zone behavior a reflection of rheological heterogeneity, Phil. Trans. R. Soc. A329: 20190421, 2021.

Fattaruso L.A., M.L. Cooke & R.J. Dorsey. 2014. Sensitivity of uplift patterns to dip of the San Andreas fault in the Coachella Valley, California. Geosphere, vol. 10, pp. 1.12.

Fuis, G. S., Scheirer, D. S., Langenheim, V. E. and Kohler, M. D.: A New Perspective on the Geometry of the San Andreas Fault in Southern California and Its Relationship to Lithospheric Structure, BSSA, 102, 236–251, 2012.

Fuis G. S., Bauer, K., Goldman, M. R., Ryberg, T., Langenheim, V. E., Scheirer, D. S., Rymer, M. J., Stock, J. M., Hole, J. A., Catchings, R. D., Graves, R. W. and Aagaard, B.: Subsurface Geometry of the San Andreas Fault in Southern California: Results from the Salton Seismic Imaging Project (SSIP) and Strong Ground Motion Expectations, BSSA, 107, 4, 1642–1662, 2017.

Guest, B., Niemi, N. and Wernicke, B.: Stateline fault system: A new component of the Miocene-Quaternary Eastern California shear zone, GSA Bull., 119, 11/12, 1337–1346, 2007.

Hardebeck J.L. & E. Hauksson. 1999. Role of fluids in faulting inferred from stress field signatures. Science, 285, pp. 236-239.

Hauksson, E., Yang, W. and Schearer, P. M.: Waveform Relocated Earthquake Catalog for Southern California (1981 to June 2011), BSSA, 102, 5, 2239–2244, 2012.

Hernandez Flores, A. P.: Paleosismologia del sistema de fallas imbricado en la Sierra Cucapah, Baja California, Mexico, Master's Thesis, Centre for Scientific Research and Higher Education, Ensenada, Mexico, 254 pp., 2015.

Herzig, C. T., Mehegan, J. M. and Stelting, C. E.: Lithostratigraphy of the State 2-14 Borehole: Salton Sea Scientific Drilling Project, J. Geophys. Res., 93, B11, 12969–l2980, 1988.

Janecke, S. U., Markowski, D. K., Evans, J. P., Persaud, P. and Kenney, M.: Durmid ladder structure and its implications for the nucleation sites of the next M >7.5 earthquake on the San Andreas fault or Brawley seismic zone in southern California, Lithosphere, 10, 5, 602–631, 2018.

Keller, E. A., Bonkowski, M. S., Korsch, R. J. and Schlemon, R. J.: Tectonic geomorphology of the San Andreas fault zone in the southern Indio Hills, Coachella Valley, California, GSA Bull., 93, 46–56, 1982.

https://doi.org/10.5194/se-2022-9
Preprint. Discussion started: 2 February 2022

Kirby, S. M., Janecke, S. U., Dorsey, R. J., Housen, B. A., Langenheim, V. E., McDougall, K. A. and Steely, A. N.: Pleistocene Brawley and Ocotillo Formations: Evidence for Initial Strike-Slip Deformation along the San Felipe and San Jacinto Fault Zones, Southern California, J. of Geology, 115, 43–62, 2007.

Leever, K., Gabrielsen, R. H., Sokoutis, D. and Willingshofer, E.: The effect of convergence angle on the kinematic evolution of strain partitioning in transpressional brittle wedges: Insight from analog modeling and high-resolution digital image analysis, Tectonics, 30, 2011a.

Leever, K., Gabrielsen, R. H., Faleide, J. I. and Braathen, A.: A transpressional origin for the West Spitsbergen fold- and thrust belt: Insight from analog modeling, Tectonics, 30, 1–24, 2011b.

Lin, G.: Three-Dimensional Seismic Velocity Structure and Precise Earthquake Relocations in the Salton Trough, Southern California, BSSA, 103, 5, 2694–2708, 2013.

Lin, G., Schearer, P. M. and Hauksson, E.: Applying a three-dimensional velocity model, waveform cross correlation, and cluster analysis to locate southern California seismicity from 1981 to 2005, J. Geophys. Res., 112, B12309, 2007.

Lindsey, E. O. and Fialko, Y.: geodetic slip rates in the southern San Andreas Fault system: Effects of elastic heterogeneity and fault geometry, J. Geophys. Res., 118, 689–697, 2013.

Lutz, A. T., Dorsey, R. J., Housen, B. A. and Janecke, S. U.: Stratigraphic record of Pleistocene faulting and basin evolution in the Borrego Badlands, San Jacinto fault zone, Southern California, GSA Bull., 118, 11/12, 1377–1397, 2006.

Markowski, D. K.: Confirmation of a New Geometric and Kinematic Model of the San Andreas Fault at Its Southern Tip, Durmid Hill, Southern California, Master's Thesis, Utak State University, Logan, USA, 151 pp., 2016.

Matti, J. C., Morton, D. M. and Cox, B. F.: Distribution and geologic relations of fault systems in the vicinity of the Central Transverse Ranges, southern California, USGS Report, 85-365, 31 pp., 1985.

McClay, K. R., Whitehouse, P. S., Dooley, T. and Richards, M.: 3D evolution of fold and thrust belts formed by oblique convergence, Mar. Petrol. Geol. Bull., 21, 857–877, 2004.

McNabb, J. C.: Stratigraphic record of Pliocene-Pleistocene basin evolution and deformation alongthe San Andreas fault, Mecca Hills, California, Unpublished Master's Thesis, University of Oregon, 70 pp., 2013.

https://doi.org/10.5194/se-2022-9
Preprint. Discussion started: 2 February 2022

McNabb, J. C., Dorsey, R. J., Housen, B. A., Dimitroff, C. and Messé, G. T.: Stratigraphic record of Pliocene–Pleistocene basin evolution and deformation within the Southern San Andreas Fault Zone, Mecca Hills, California, Tectonophys., 719–720, 66–85, 2017.

Miller, D.D.: Distributed shear, rotation, and partitioned strain along the San Andreas fault, central California, Geology, 26, 867–870, 1998.

Morton, D., Matti, J. and Tinsley, J.: Banning fault, Cottonwood canyon, San Gorgonio pass, southern California, in: Cordilleran Section of the Geological Society of America, edited by: Hill, M., 191–192, Geol. Soc. of Am., Boulder, Colorado, USA, 1987.

Mount, V. S. and Suppe, J.: State of stress near the San Andreas fault: implications for wrench tectonics, Geology, 15, 1143–1146, 1987.

Nicholson, C., Hauksson, E. and Plesch, A.: Revised 3D Fault Models for the Southern San Andreas Fault System Extending from San Gorgonio Pass to the Salton Sea, 106th Annual Meeting AAPG, 27th–29th May, 2010.

Nur, A., Hagai, R. and Beroza, G. C.: The Nature of the Landers-Mojave Earthquake Line, Science, 261, 201–203, 1993a.

Nur, A., Hagai, R. and Beroza, G. C.: Landers-Mojave earthquake Line: A New Fault System?, GSA Today, 3, 10, 255–258, 1993b.

Parrish, J.G.: Geological compilation of Quaternary surficial deposits in southern California, Palm Springs 30’ x 60’ quadrangle, CGS Special Report 217, Plate 24, 1983.

Platt, J. P. and Passchier, C. W.: Zipper junctions: A new approach to the intersections of conjugate strike-slip faults, Geology, 44, 10, 795–798, 2016.

Rymer, M. J.: Quaternary Fault-Normal Thrusting in the Northwestern Mecca Hills, Southern California, GSA Cordilleran Section Guidebook, Trip 15, 268–272, 1994.

Sanderson, D. J. and Marchini, W. R. D.: Transpression, J. Structural Geol., 6, 5, 449–458, 1984.

Sarna-Wojcicki, A. M., Pringle, M. S. and Wijbrans, J.: New ^{40}Ar/^{39}Ar age of the Bishop Tuff from multiple sites and sediment rate calibration for the Matuyama-Brunhes boundary, J. Geophys. Res., 105, B9, 21431–21443, 2000.

Schlische, R. W.: Geometry and origin of fault-related folds in extensional settings, AAPG Bull., 79, 1661–1678, 1995.

Schultz, R. A. and Balasko, C. M.: Growth of deformation bands into echelon and ladder geometries, Geophys. Res. Lett., 30, 2033, 2003.

https://doi.org/10.5194/se-2022-9
Preprint. Discussion started: 2 February 2022

Sheridan, J. M. and Weldon II, R. J.: Accomodation of compression in the Mecca Hills, California, GSA Cordilleran Section Guidebook, Trip 15, 273–279, 1994.

Sheridan, J. M., Weldon II, R. J., Thornton, C. A. and Rymer, M. J.: Stratigraphy and Deformational History of the Mecca Hills, Southern California, GSA Cordilleran Section Guidebook, Trip 15, 262–268, 1994.

Spinler, J. C., Bennett, R. A., Anderson, M. L., McGill, S. F., Hreinsdottir, S. and McCallister, A.: Present-day strain accumulation and slip rates associated with southern San Andreas and eastern California shear zone faults, J. Geophys. Res., 115, B11407, 2010.

Spotila, J. A., Niemi, N., Brady, R., House, M., Buscher, J and Oskin, M.: Long-term continental deformation associated with transpressive plate motion: The San Andreas fault, Geology, 35, 11, 967–970, 2007.

Sylvester, A. G.: Strike-slip faults, GSA Bull., 100, 1666–1703, 1988.

Sylvester, A. G. and Smith, R. R.: Tectonic Transpression and Basement-Controlled Deformation in San Andreas Fault Zone, Salton Trough, California, Treatise of Petroleum Geology, 60, 12, 2081–2102, 1976.

Sylvester, A. G. and Smith, R. R.: Structure section in Painted Canyon, Mecca Hills, southern California, GSA Centennial Field Guide, Cordilleran Section, 103–108, 1987.

Sylvester, A. G., Bilham, R., Jackson, M. and Barrientos, S.: Aseismic Growth of Durmid Hill, Southeasternmost San Andreas Fault, California, J. Geophys. Res., 98, B8, 14233–14243, 1993.

Titus, S. J., Housen, B. and Tikoff, B.: A kinematic model for the Rinconada fault system in central California based on structural analysis of en echelon folds and paleomagnetism, J. Struct. Geol., 29, 961–982, 2007.

Thatcher, W., Savage, J. C. and Simpson, R. W.: The Eastern California Shear Zone as the northward extension of the southern San Andreas Fault, J. Geophys. Res., Solid Earth, 121, 2904–2914, 2016.

Tyley, S. J.: Analog model study of the ground-water basin of the upper Coachella Valley, California, U.S. Geological Survey Water-Supply, 2027, 1974.

Winker, C. D. and Kidwell, S. M.: Stratigraphy of a marine rift basin: Neogene of the western Salton Trough, California, in: Field Conference Guide, edited by: Abbott, P. L. and Cooper, J. D., AAPG National Convention, San Diego, California, USA, 295–336, 1996.

Zeeden, C., Rivera, T. A. and Storey, M.: An astronomical age for the Bishop Tuff and concordance with radioisotopic dates, Geophys. Res. Lett., 41, 3478–3484, 2014.

https://doi.org/10.5194/se-2022-9
Preprint. Discussion started: 2 February 2022

Figures

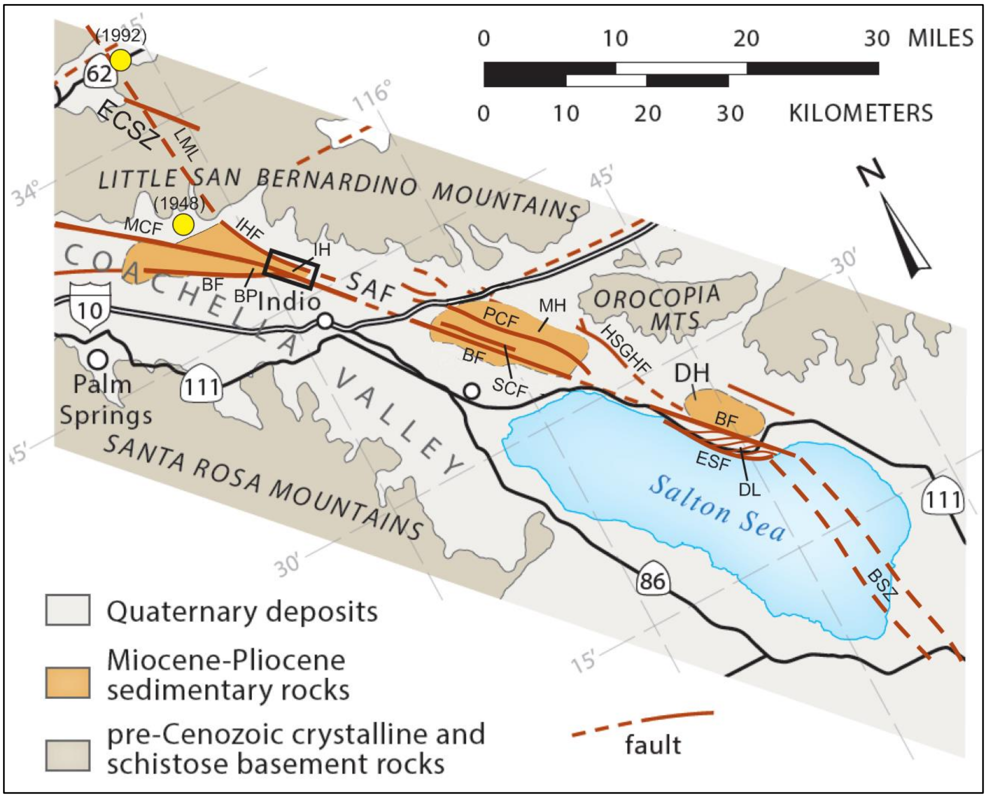

Figure 1: Simplified geological map of the Coachella Valley and Salton Trough, southern California, showing the three main transpressional uplift areas along the SAFZ: the Indio Hills (IH), Mecca Hills (MH), and Durmid Hills (DH). Note the link of the SAFZ with the Brawley seismic zone to the south. The study area is shown in a black rectangle. Recent earthquakes (< 75 years) along the Landers–Mojave Line (LML) are shown as yellow dots with associated year of occurrence in parenthesis. Abbreviations: BF: Banning Fault; BP: Biskra Palms; DL: Durmid ladder; ECSZ: East California Shear Zone; ESF: Eastern Shoreline Fault; HSGHF: Hidden Springs–Grotto Hills fault; IHF: Indio Hills fault; LML: Landers–Mojave Line; MCF: Mission Creek Fault; PCF: Painted Canyon Fault; SCF: Skeleton Canyon Fault. Modified after Bergh et al. (2019).

https://doi.org/10.5194/se-2022-9
Preprint. Discussion started: 2 February 2022

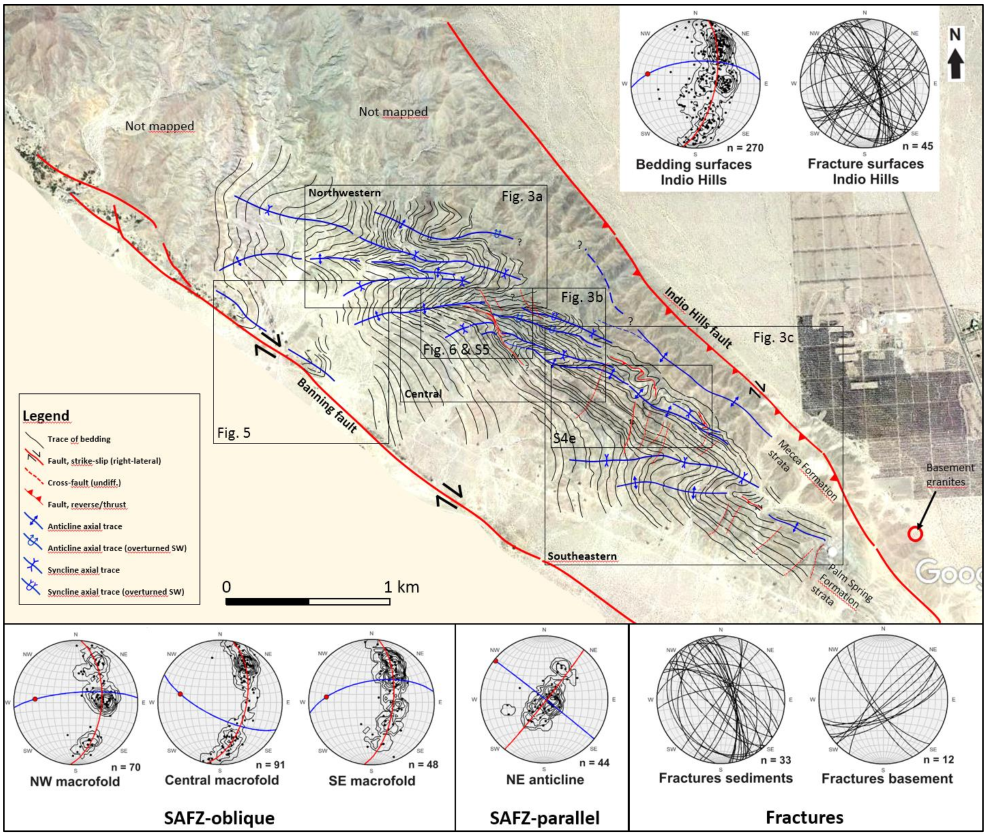

Figure 2: Interpreted DEM image in the southeasternmost part of the Indio Hills uplift area. Three main SAFZ-oblique macro-folds (northwestern, central, southeastern) are mapped in between the bounding Indio Hills and Banning faults, whereas one SAFZ-parallel anticline is present close to the Indio Hills fault. More detailed figures are numbered and framed. Structural datasets are plotted in lower hemisphere Schmidt stereonets. Bedding surfaces are shown as pole to plane with frequency contour lines, with average πS great circle (red great circles), fold axial surface (blue great circles) and fold axis (red dots). Brittle fractures in sedimentary strata and basement rocks are plotted as great circles. Source: Google Earth historical imagery 09-2011. © Google Earth 2011.

https://doi.org/10.5194/se-2022-9
Preprint. Discussion started: 2 February 2022

Solid Earth
Discussions

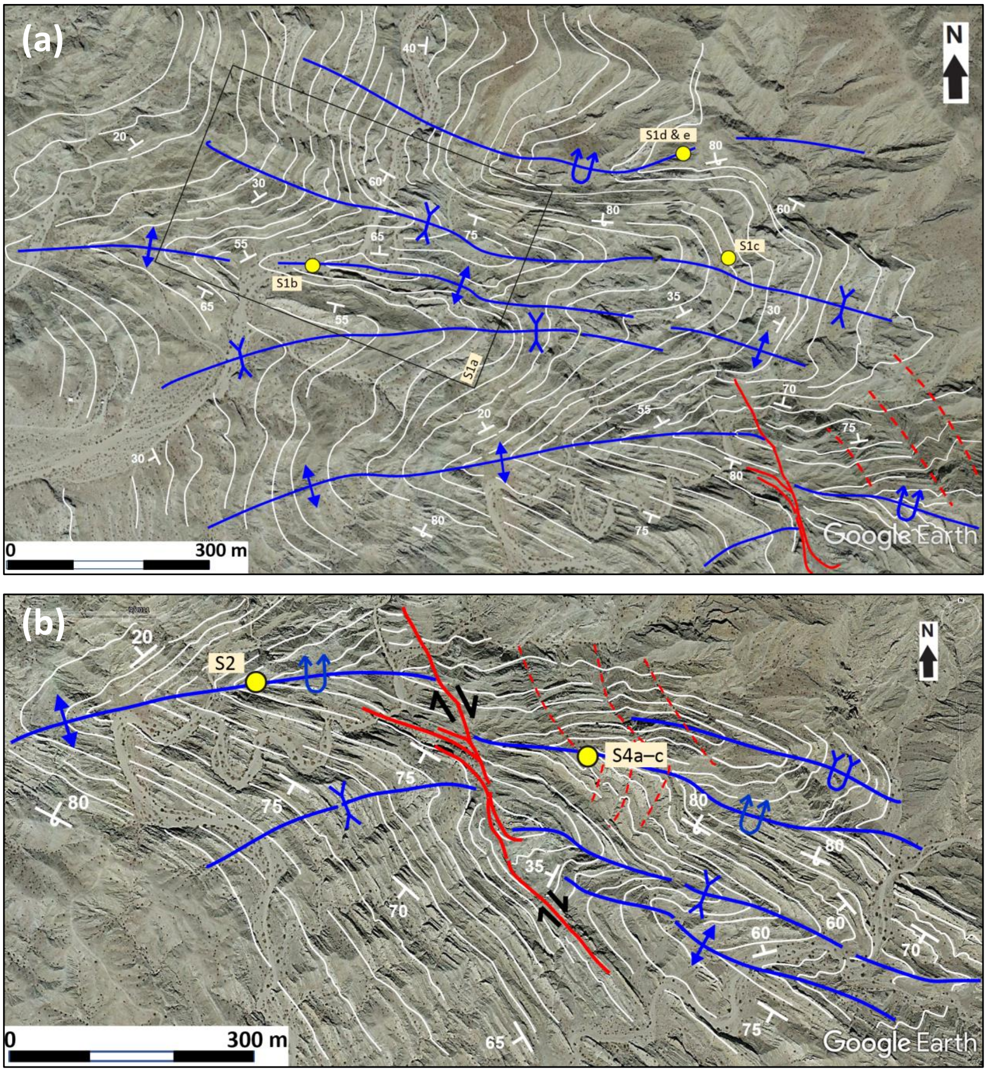

https://doi.org/10.5194/se-2022-9
Preprint. Discussion started: 2 February 2022

Solid Earth Discussions
Open Access

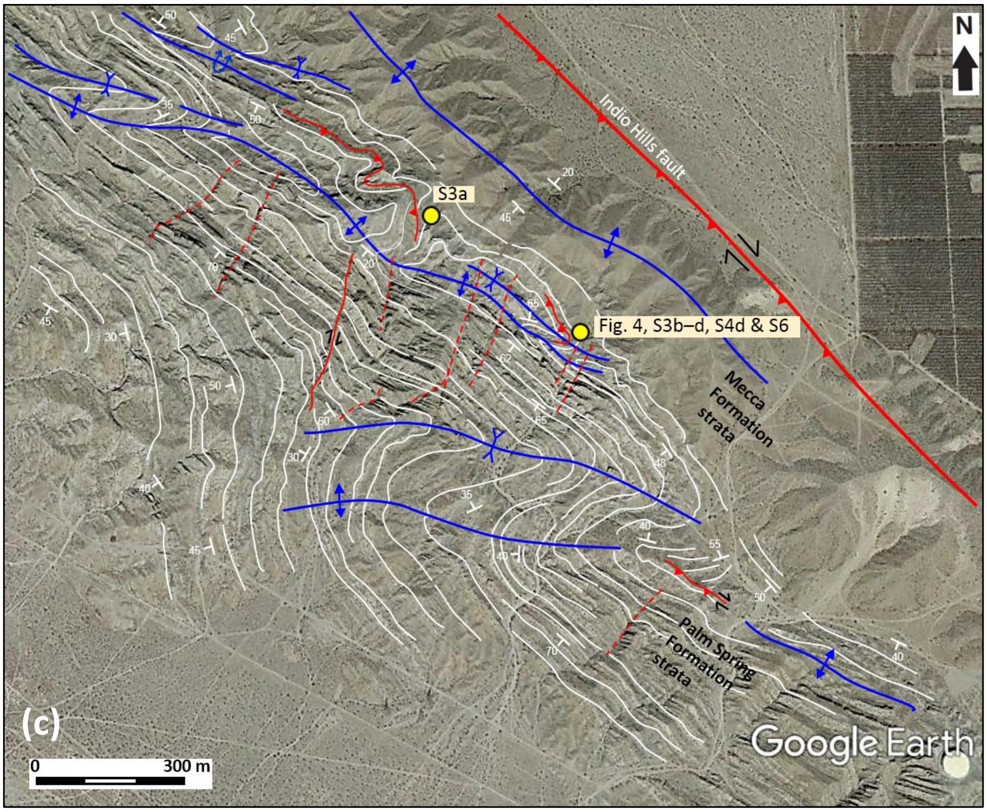

Figure 3: Detailed structural maps showing the architecture and outline of anticline-syncline pairs, traces of bedding and strike and dip orientation, axial surface traces, and fold-related faults in (a) the northwestern, (b) central, and (c) southeastern macro-folds. Note tighter and consistently asymmetric (Z-shaped) geometries of the macro-folds to the east, whereas folds to the west are more open and symmetric. Traces and orientation of bedding show a back-limb composed of attenuated shear folds merging from the central macro-fold in the north, whereas the forelimb is much shorter and more regularly folded. See fig. 2 for legend and location. © Google Earth 2011.

https://doi.org/10.5194/se-2022-9
Preprint. Discussion started: 2 February 2022

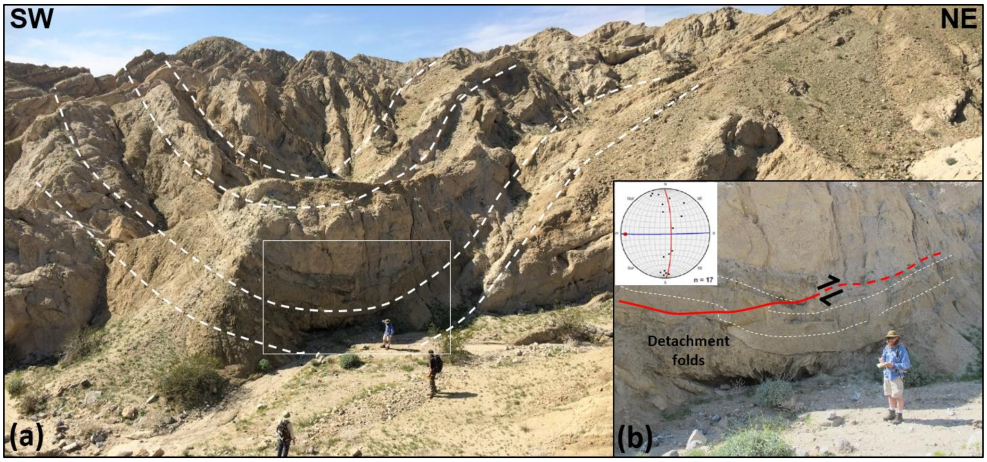

Figure 4: Meso-scale folds and related faults on the back-limb of the southeastern macro-fold. See location in fig. 3c. (a) Syncline in upper Palm Spring Formation units adjacent to the SAFZ-parallel macro-fold near the Indio Hills fault. (b) Close-up view of the synclinal fold hinge in (a), where a meter thick sandstone bed is slightly offset by a minor, low-angle thrust fault (red line) with NE-directed sense-of-shear. The minor thrust faults die out in the overlying sandstone bed. The mudstone bed below acts as a décollement layer with internal, plastically folded lamination, including disharmonic folds. Structural orientation data of minor fold limbs in the décollement zone are plotted in a lower hemisphere Schmidt stereonet, indicating E–W-trending fold axes and a sub-horizontal axial surface (average great circle in red and fold axis as a red dot).

https://doi.org/10.5194/se-2022-9
Preprint. Discussion started: 2 February 2022

Solid Earth
Discussions
Open Access

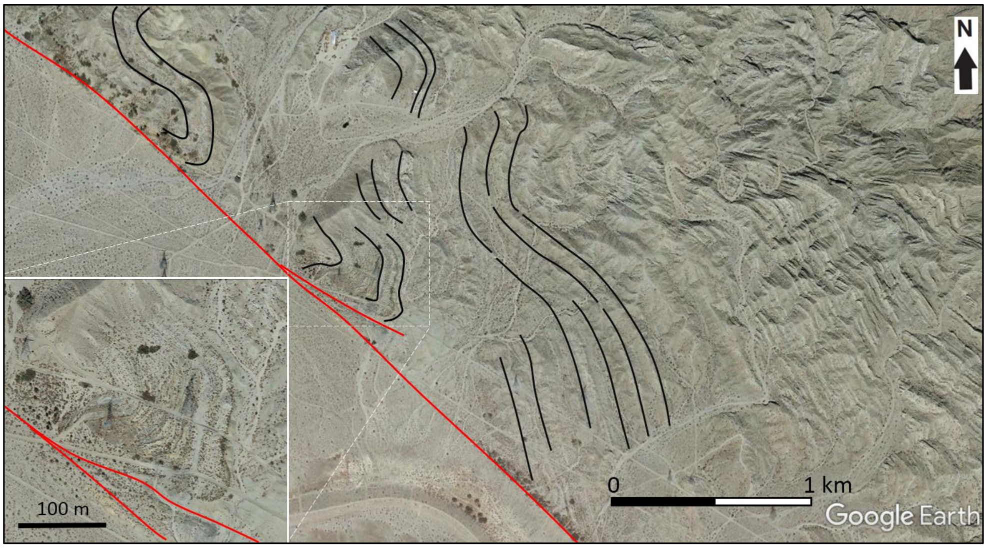

Figure 5: Interpreted SAFZ-parallel macro-folds adjacent to the Banning fault, which affect the southern limb of earlier (*en echelon*) macro-folded and tilted strata of the Palm Spring Formation. Note shear fold geometry in inset map with a thickened hinge zone and thinned limb to the south, and a steeply plunging axis. See fig. 2 for location. © Google Earth 2011.

https://doi.org/10.5194/se-2022-9
Preprint. Discussion started: 2 February 2022

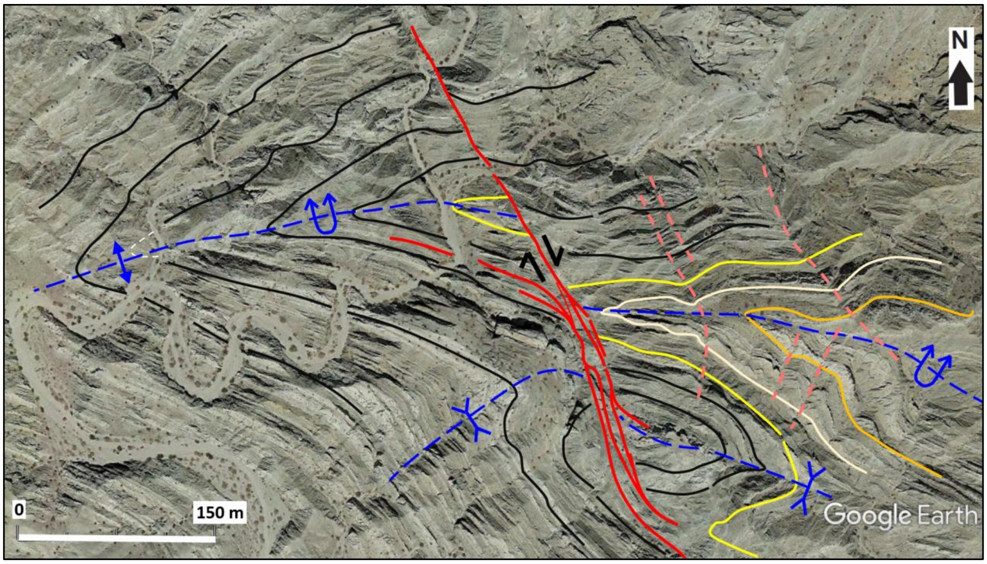

Figure 6: Interpreted satellite image of the central macro-fold showing right-lateral offset of the entire fold hinge/axial surface (upper left dashed blue line) by a NNW–SSE-trending, NE-dipping strike-slip fault (red lines). Note that the fault merges out from a layer in the southern limb of the macro-fold (black lines) and continues as a right-lateral fault. Offset geological markers include thick sandstone beds (yellow, white, light brown lines) and the fold axial surfaces of a second syncline fold farther south (lower right, dashed blue lines). Note that the syncline axial trace dies out to the southwest, and that kink bands acting as cross faults crop out in the eastern part of image (dashed pink lines). Uninterpreted version of the image available as Supplement S5. © Google Earth 2011.

https://doi.org/10.5194/se-2022-9
Preprint. Discussion started: 2 February 2022

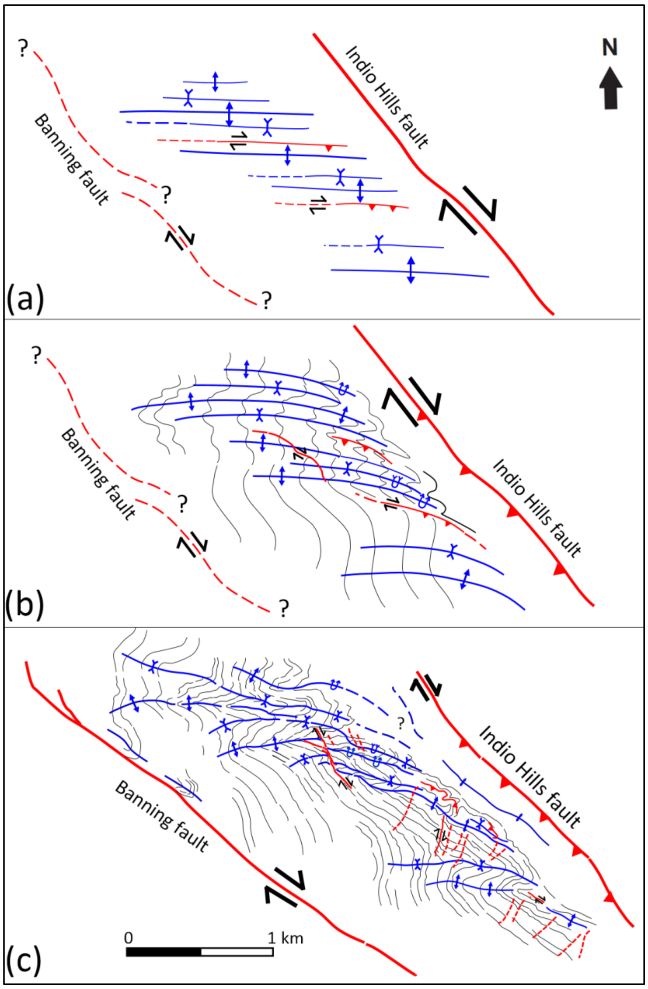

Figure 7: Tentative model illustrating the progressive uplift/inversion history of the Indio Hills presuming a narrow time interval between formation of all structures in the area, except for the Banning fault and associated folds. (a) Early distributed transpressional strain and formation of three major, en-echelon oriented macro-folds, several subsidiary parasitic anticline-syncline fold pairs, and bed-parallel strike-slip and reverse (décollement) faults at a high angle (c. 45°) to the Indio Hills fault. (b) Incremental partly partitioned transpression when the Indio Hills fault started to accommodate oblique-reverse movement forcing previous horizontal *en echelon* macro-folds and parasitic folds to tighten, overturn, and rotate into steeper westward plunges. Note also sigmoidal rotation of axial traces on the back-limbs of the macro-folds to low angle (< 20–30°) with the Indio Hills fault. (c) Late-stage advanced strain partitioning

https://doi.org/10.5194/se-2022-9
Preprint. Discussion started: 2 February 2022

with dominant shortening component on the oblique-reverse Indio Hills fault, and right-lateral slip on the Banning Fault. Notice the formation of the anticline parallel to the Indio Hills fault, subsidiary fold-internal strike-slip faults, and conjugate cross faults and kink bands that overprinted the macro-folds. Legend as in fig. 2.

https://doi.org/10.5194/se-2022-9
Preprint. Discussion started: 2 February 2022

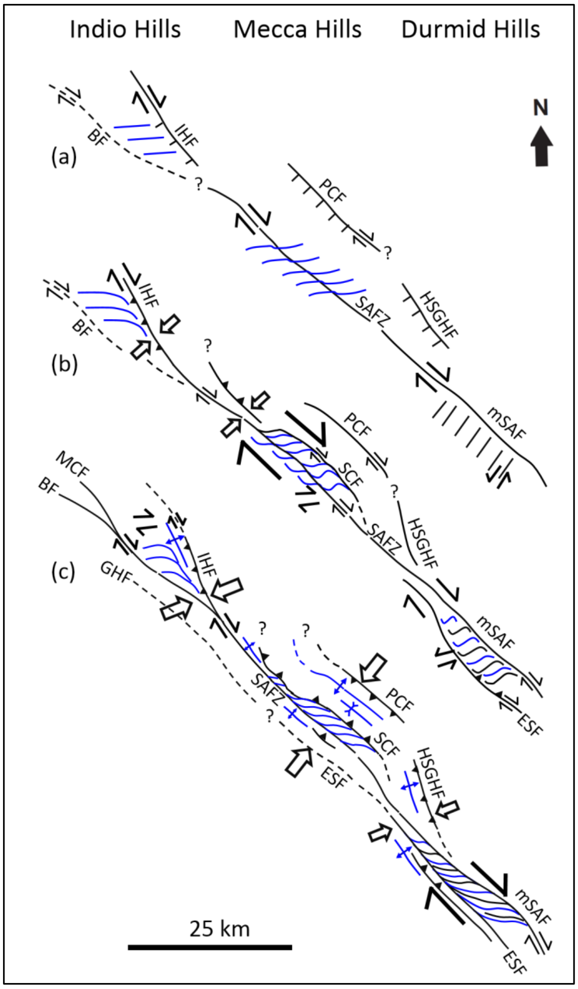

Figure 8: Kinematic evolution and along-strike correlation of the Indio Hills, Mecca Hills, and Durmid Hills uplift domains and bounding master faults in the Coachella valley, southern California. We present a progressive kinematic evolution from (a) distributed, through (b) partly partitioned, to (c) advanced partitioned strain events. See text for further explanation. Black lines are faults (full or stippled). Blue lines are fold axial traces. Wide arrows indicate main shortening direction, half-arrows lateral (strike-slip) shearing. Abbreviations: BF: Banning fault; ESF: Eastern Shoreline fault; GHF: Garnet Hills fault; HSGHF: Hidden Springs–Grotto Hills fault; IHF: Indio Hills fault; mSAF: main San Andreas fault in Durmid Hills; MCF: Mission Creek fault; PCF: Painted Canyon fault; SAFZ: San Andreas transform fault; SCF: Skeleton Canyon fault.